URSI GASS 2023, Sapporo, Japan, 19 – 26 August 2023

Automated Test Setup for Capacitive Power Transfer Coupler Impedance Measurements

Cédric Lecluyse[(1)]*, Kiran Peirens[(1)], Simon Ravyts[(1)], Peter Bracke [(1)], Ben Minnaert[(2)], Michael Kleemann[(1)]
(1) KU Leuven, ELECTA Ghent, Ghent 9000, Belgium
(2) University of Antwerp, Cosys-Lab, Antwerp 2020, Belgium

Abstract

Capacitive power transfer is an emerging technology of which some parameters have not yet been sufficiently investigated. This article proposes an automated test setup to experimentally determine the key parameters, such as capacitance and leakage resistance, of a capacitive power transfer coupler. Using the results, the potential of capacitive power transfer in terms of, for instance, transferable power for a given distance, are revealed and theoretic models can be validated. An exemplary experiment shows that 5 mm plexiglass has a seven times greater leakage resistance than a 5 mm air gap.

1 Introduction

Wireless power transfer (WPT) is a worthy alternative to conductive charging for applications such as smartphones and electric vehicles (EVs). WPT uses electromagnetic fields to transfer power between a transmitter and receiver. For the previously mentioned applications, charging smartphones or EVs, it is referred to as near-field WPT. Here, the distance between the transmitter and receiver is less than the wavelength of the electromagnetic fields. One near-field technology is capacitive power transfer (CPT) which uses electric fields to transfer energy between metal plates. CPT has been in the focus of research for about a decade because of the advantages it offers. For instance, it can be manufactured with cheap and light metal plates and is less affected by nearby metal objects.

At an earlier research stage, the plate structure of the coupler was researched but mainly with air as medium between the transmitter and receiver [1, 2]. Subsequently, research evolved towards the inverter and compensation circuits [3]. However, there is still a lack of knowledge about the influence of the material between the coupler plates on power transmission as well as what losses the material entails. To determine and measure the parameters that affect this, an automated measurement setup is needed.

The literature on capacitive power transfer generally refers to the four parallel plate structure. As can be seen from Fig. 1, an idealized CPT system consists of two parallel plate capacitors in series. In practical terms, other parasitic components are involved. The state of research is limited to a power transfer through air, which is idealized with no other parasitic components than the parasitic capacitances between the plates. To the best of our knowledge, there is no data available about the other parasitic components such as the leakage resistance of solid media such bricks or insulation. This lack of data forms a burden for validating theoretic models and implementing simulations. To quantify those parasitic components, a practical measurement setup is needed.

First, this paper describes the most important parameters of CPT: the coupler capacitance, and the leakage resistance. Next, the automated setup is reported. Finally, experimental results are shown, comparing air and plexiglass as medium.

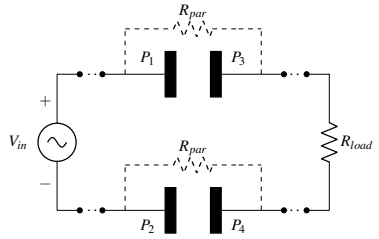

Figure 1. Four plate CPT coupler

2 Capacitive power transfer parameters

2.1 Coupler capacitance

A typical four plate structure, as shown in Fig. 1, contains two main capacitances C_{13} & C_{24} and parasitic components such as the two cross-coupling capacitances C_{14} & C_{23} and two leakage capacitances C_{12} and C_{34}. This circuit is simplified to the Pi model represented by the primary capacitance C_p, secondary capacitance C_s and mutual capacitance C_m [1].

If the CPT setup is symmetrical ($C_{main} = C_{13} = C_{24}$), and the distance between transmitter and receiver is smaller than e.g. 20 mm, the following assumptions can be made [4]. The cross-coupling and parasitic capacitances are negligible making the mutual C_M, primary C_P and secondary C_S capacitances equal to half of C_{13} and C_{24} [1]. This ensures perfect coupling between primary and secondary. These assumptions allow the capacitance value of

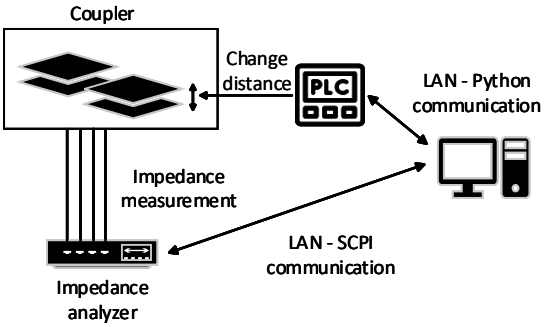

(a)

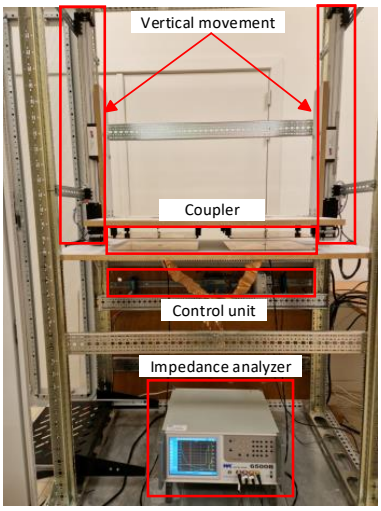

(b)

Figure 2. (a): Block diagram of the practical setup; (b): Practical setup of CPT impedance measurements

the coupler to be determined using the simplest capacitor equation (1):

$$C_{main} = \varepsilon_0 \cdot \varepsilon_r \cdot \frac{A}{d} \tag{1}$$

In this equation, three parameters govern the capacitance of the CPT coupler. First, the area of the coupler, represented by A. Second, the distance between the plates, represented by d. Third, the dielectric material properties represented by ε_0, which represents the permittivity in vacuum, and ε_r, which represents the relative permittivity, which is material-dependent. Equation (1) can be used for CPT systems with two parallel plates in series. This approximates the capacitance for a CPT system quite well for symmetrical systems bridging distances of less than 20 mm [4]. However, this approximation does not take into account the influence of the frequency of the electrical field between the plates. However, frequency-dependent fringing effects or dipole losses do occur above several hundreds of kilohertz [5–7].

2.2 Leakage resistance

In this section, frequency dependent effects are taken into account to obtain a more accurate approximation of the leakage resistance. When considering equation (1), the relative permittivity is expressed by a real number. A more accurate representation consists of a real and imaginary part, represented as follows:

$$\varepsilon_r = \varepsilon_r' + j \cdot \varepsilon_r'' \tag{2}$$

The real part ε_r' provides the phase shift of the electric field while the imaginary part represents the losses in the material. These dielectric losses are caused by oriental polarization, which occurs mainly in materials with a permanent dipole moment. The electric field causes a reorientation of the dipoles at frequency of the field. With the rotation of the dipoles comes friction, which causes losses [7]. These losses are denoted in Fig.1 as R_{par}. Using equation (2), the theoretical impedance of the coupler is described by equation (3).

$$Z_{system} = \frac{\varepsilon_r'' - j \cdot \varepsilon_r'}{\omega \cdot C_0 \cdot (\varepsilon_r'^2 + \varepsilon_r''^2)} \tag{3}$$

Unfortunately, there is a lack of experimental data on ε_r'' for different materials in the frequency range of CPT. Therefore, experimental data needs to be gathered to make use of equation (3). For this, an experimental setup needs to be designed.

3 Practical setup

In this section, a practical setup is developed to experimentally explore the CPT key parameters and to determine its frequency-dependent permittivity. To obtain valid measurements the setup must be able to change the plate distance automatically, with a 0.1 mm accuracy, to allow measurements taking several minutes or hours without user interaction. Furthermore, the coupler impedance must be measured for a frequency range from 500 kHz to 15 MHz, considering current power electronic inverter technology. Fig. 2a shows the schematic representation of the practical setup in Fig. 2b. The main components to build this setup are listed in Table 1.

Table 1. Main components of the setup

Goal	Device	Specification
Plate movement	2x Nanotec NEMA23 2x BAHR ELK40	range: 1 - 300 mm accuracy: 0.1 mm
Impedance measurement	Wayne Kerr 6500B	20 Hz - 120 MHz accuracy: 0.05 % SCPI communication
Automation	Siemens S7 1214C DC/DC/DC Computer	TIA portal - Python

3.1 Automated setup

Automation of the setup is one of the key requirements to ensure that measurements are performed under the same conditions. The corresponding control flow is shown in Fig. 3 This is realized by using a user-controlled python script that communicates via LAN with a PLC and an impedance analyzer. The PLC is used to control the stepper motors via their motor controller. When the stepper motors have reached their requested position, the python script communicates to the impedance analyzer that it can start the impedance measurements over the set frequency sweep. When the impedance measurements are complete, the python script gives the command to move to the next distance or, at the end after all the measurements, to export the measurement data to a CSV file.

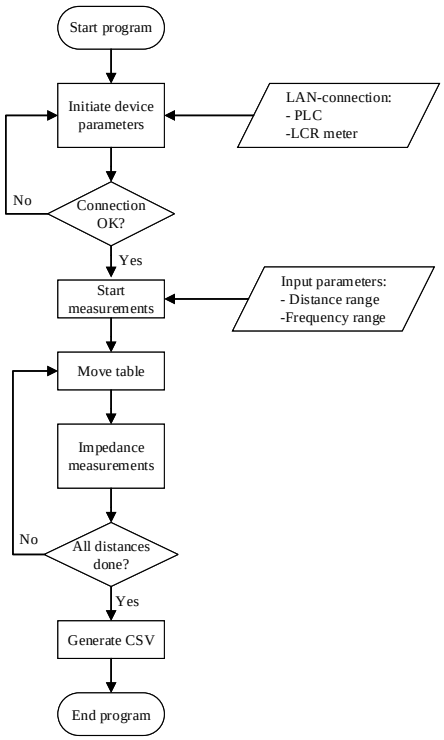

Figure 3. Flowchart of automated CPT impedance measurements

4 Experimental results

Before measurements are started, the system is calibrated to minimize external influences. For this, the impedance analyzer requires an open and short circuit calibration as well as a high frequency calibration to compensate for the influence of cables on the measurement circuit. This calibration should be performed without the transmitter and receiver plates as they are part of the measurements. Furthermore, an additional short circuit and open circuit measurement is required with transmitter and receiver plates to measure the parasitic components of the plates. This is later processed in the analysis so that only the influence of the medium is measured.

For measurements performed with an impedance analyzer, the secondary side of the CPT coupler is short-circuited as shown in Fig. 4. As a result of the symmetrical system, half of the mutual impedance is measured. When translated into the mutual capacitance C_m and the leakage resistance R_m, it is twice the mutual capacitance C_m and thus equals to the main capacitance C_{main} or equals to C_{13} and C_{24}.

$$Z_{system} = \frac{Z_m}{2} = \frac{R_m + j \cdot X_m}{2} = \frac{R_m}{2} - \frac{j}{\omega \cdot 2 \cdot C_m} = \frac{R_m}{2} - \frac{j}{\omega \cdot C_{main}} \tag{4}$$

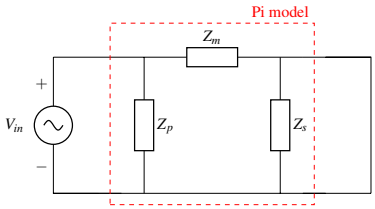

Figure 4. Short circuit CPT pi model

4.1 Capacitance measurements

Using the measurement setup, the coupler capacitance is measured automatically as function of frequency and distance between the plates. Because of this, it is possible to obtain 3D figures, as shown in Fig. 5.

For small distances, up to about 10 mm, irregularities can be seen on the figure. This is due to resonance occurring at that distance and frequency. As the distance between the plates increases, it is noticeable that the capacitance decreases as well as that no resonance phenomena occur below 15 MHz, as was expected from equation (1). Furthermore, it can be seen on Fig. 5 that as the frequency of the field increases, the coupler capacitance also increases as the frequency approaches the resonant frequency.

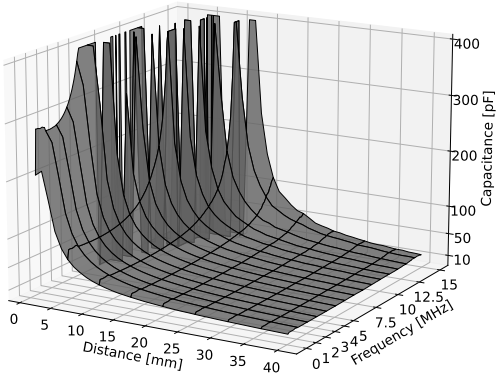

Figure 5. Capacitance measurement for distance and frequency sweep

4.2 Leakage resistance measurements

Fig. 5 shows 2 measurements of the leakage resistance for a 5 mm air gap and 5 mm thick plexiglass plate. Using this measurement, it can already be disproved that no losses occur in capacitive power transfer with air as medium. Within a typical frequency range of capacitive power transfer, between 500 kHz and 6.78 MHz, the leakage resistance in air is between 3.3 and 1.5 Ω. This is comparable to the ESR of a 12 pF film dielectric trimmer [8]. When a 5 mm air gap is compared with 5 mm plexiglass plate as medium, it is noticeable that at 1 MHz the leakage resistance of plexiglass is about seven times higher while the relative permittivity of plexiglass is about three times the relative permittivity of air.

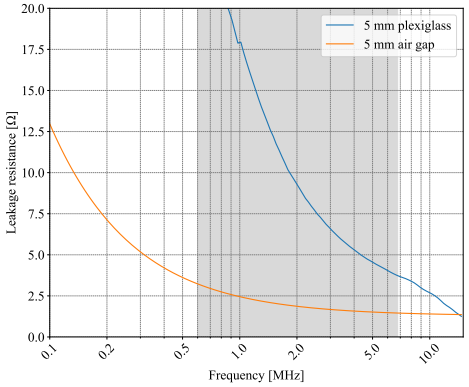

Figure 6. Leakage resistance measurements of 5 mm plexiglass and 5 mm air gap as medium

5 Conclusion

This paper develops an automated setup to explore a four-plate capacitive power transfer coupler. This is necessary due to the fact that the measured values are highly dependent on frequency of the electric field and distance between the plates. These measurements make it possible to determine both the resulting capacitance value and the leakage resistance of a capacitive power transfer coupler. First experimental results show that dielectric losses are not negligible for air. Also, the dielectric losses in plexiglass are seven times greater than the losses in air while the coupling capacity is only three times greater. In the future, this setup will be used to explore various solid media for capacitive power transfer. This will provide data that the state of research is lacking and allows for the validation of theoretic frequency-dependent CPT models. The setup will be further extended to a configuration where an inverter is connected to the primary side. By connecting a load at the secondary side, the influence of the medium on the power transfer can be measured as well as the losses that occur.

References

[1] C. Lecluyse, B. Minnaert, and M. Kleemann, "A review of the current state of technology of capacitive wireless power transfer," *Energies*, vol. 14, no. 18, 2021.

[2] H. Zhang, F. Lu, H. Hofmann, W. Liu, and C. C. Mi, "Six-plate capacitive coupler to reduce electric field emission in large air-gap capacitive power transfer," *IEEE Transactions on Power Electronics*, vol. 33, no. 1, pp. 665–675, 2018.

[3] D. Rozario, N. A. Azeez, and S. S. Williamson, "Comprehensive review and comparative analysis of compensation networks for capacitive power transfer systems," in *2016 IEEE 25th International Symposium on Industrial Electronics (ISIE)*, pp. 823–829, 2016.

[4] C. Lecluyse, B. Minnaert, S. Ravyts, and M. Kleemann, "Influence of a medium on capacitive power transfer capability," in *2022 Wireless Power Week (WPW)*, pp. 589–594, 2022.

[5] H. Nishiyama and M. Nakamura, "Form and capacitance of parallel-plate capacitors," *IEEE Transactions on Components, Packaging, and Manufacturing Technology: Part A*, vol. 17, no. 3, pp. 477–484, 1994.

[6] X. Chen, Z. Zhang, S. Yu, and T.-G. Zsurzsan, "Fringing effect analysis of parallel plate capacitors for capacitive power transfer application," pp. 1–5, 2019.

[7] M. Mehdizadeh, "Chapter 1 - the impact of fields on materials at microwave and radio frequencies," in *Microwave/RF Applicators and Probes (Second Edition)* (M. Mehdizadeh, ed.), pp. 1–33, Boston: William Andrew Publishing, second edition ed., 2015.

[8] Vishay BCcomponents, *Film Dielectric Trimmers*, 2012.